

## Supplementary Information

### **Accelerated and controlled polymerization of *N*-carboxyanhydrides assisted by acids**

Xingliang Liu,<sup>1,4, #</sup> Jing Huang,<sup>1,4, #</sup> Jiaqi Wang<sup>1</sup>, Haonan Sheng<sup>1</sup>, Zhen Yuan<sup>1</sup>,  
Wanying Wang<sup>3</sup>, Wenbin Li<sup>1</sup>, Ziyuan Song,<sup>3, \*</sup> and Jianjun Cheng<sup>1,2,4, \*</sup>

<sup>1</sup>School of Engineering, Westlake University, Hangzhou 310030

<sup>2</sup>Research Center for Industries of the Future, Westlake University, Hangzhou 310030

<sup>3</sup>Institute of Functional Nano & Soft Materials (FUNSOM), Jiangsu Key Laboratory for Carbon-Based Functional Materials and Devices, Soochow University, Suzhou 215123

<sup>4</sup>Institute of Advanced Technology, Westlake Institute for Advanced Study, Hangzhou, Zhejiang 310024

\*Corresponding email: chengjianjun@westlake.edu.cn, zysong@suda.edu.cn

## Table of Contents

Materials .....	S3
Instrumentations.....	S3
Polymerization kinetics.....	S4
Simulation Methods.....	S4
Supporting Figures.....	S6
Supporting Tables .....	S33
Cartesian Coordinates of the optimized geometries .....	S41
Supporting References .....	S59

## Materials

All commercial reagents were purchased from Shanghai Aladdin Biochemical Technology Co., Ltd. (Shanghai, China) and used as received unless otherwise specified. Amino acids, 18-crown 6-ether (CE), tetrabutylammonium acetate (TBAA) and *N,N'*-bis[3,5-bis(trifluoromethyl)phenyl]thiourea (TU-S) were purchased from Tokyo Chemical Industry (Shanghai, China). Triphosgene and maleic anhydride were purchased from Shanghai Macklin Biochemical Technology Co., Ltd. (Shanghai, China). The initiator *n*-hexylamine (Hex-NH<sub>2</sub>) was purchased from Millipore Sigma Chemical Co. (St. Louis, MO, USA). Deuterated solvents were purchased from Cambridge Isotope Laboratories, Inc. (Tewksbury, MA, USA). Monomers including  $\gamma$ -benzyl-L-glutamate *N*-carboxyanhydride (BLG-NCA),  $\gamma$ -ethyl-L-glutamate *N*-carboxyanhydride (ELG-NCA),  $\gamma$ -(4-propargyloxy)benzyl-L-glutamate NCA (POB-NCA), *N*<sup>ε</sup>-carboxybenzyl-L-lysine NCA (ZLL-NCA), and  $\alpha,\gamma$ -dibenzyl-L-glutamate (DBLG) were synthesized following literature procedures.<sup>1-3</sup>

## Instrumentations

<sup>1</sup>H nuclear magnetic resonance (<sup>1</sup>H NMR) spectra were recorded on a 600 MHz-Solution NMR Spectrometer, Westlake University. Chemical shifts ( $\delta$ ) were reported in ppm and referenced to the residual protons in deuterated solvents. MestReNova software (version 14.0.0, Mestrelab Research, Escondido, CA, USA) was used for all NMR analysis. Gel permeation chromatography (GPC) experiments were performed on a system equipped with an isocratic pump (1260 Infinity II, Agilent, Santa Clara, CA, USA), a multi-angle static light scattering (MALS) detector (DAWN HELEOS-II, Wyatt Technology, Santa Barbara, CA, USA), and a differential refractometer (dRI) detector (Optilab, Wyatt Technology, Santa Barbara, CA, USA). The detection wavelength of HELEOS was set at 658 nm. Separations were performed using serially connected size exclusion columns (three Shodex<sup>TM</sup> packed columns KD-803, KD-804 and KD-805, 10  $\mu$ m, 8  $\times$  300 mm, Yokohama, Japan) using *N,N*-dimethylformamide (DMF) containing LiBr (0.1 mol/L) as the mobile phase at a flow rate of 1.0 mL/min at 50 °C. The MALS detector was calibrated using pure toluene and can be used for the determination of the absolute molecular weights (MWs). The MWs of polymers were determined based on the  $dn/dc$  value of each polymer sample using the internal calibration system processed by the ASTRA 8.1.2 software (version 8.12, Wyatt Technology, Santa Barbara, CA, USA). Fourier transform infrared (FTIR) spectra were

recorded on a Perkin Elmer 100 serial FTIR spectrophotometer (PerkinElmer, Santa Clara, CA, USA) calibrated with polystyrene film. Matrix-assisted laser desorption/ionization time-of-flight (MALDI-TOF) mass spectra were collected on a Bruker Rapiflex in the mass spectrometry laboratory, Westlake University, with *trans*-2-[3-(4-*tert*-butylphenyl)-2-methyl-2-propenylidene] malononitrile (DCTB) as the matrix. Circular dichroism (CD) data was collected using a chirascan spectrometer V100 (Applied Photophysics, Leatherhead, UK). The pathlength of the CD cuvette was 0.5 mm.

### **Polymerization kinetics**

For the polymerization kinetic experiment, the consumption of NCA was monitored through FTIR or NMR. In a typical FTIR experiment, the polymerization mixture was transferred into a liquid FTIR cell after the mixing of monomer, initiator, and acid. The FTIR spectra were monitored at different time intervals until the disappearance of anhydride peaks from NCA at 1860  $\text{cm}^{-1}$  and 1790  $\text{cm}^{-1}$ . The concentration of NCA monomer was then quantified through the standard curve based on the absorbance at 1790  $\text{cm}^{-1}$ .

Similarly, the polymerization kinetics was also monitored in situ by  $^1\text{H}$  NMR in deuterated solvent in an NMR tube. The conversions of NCA were quantified by monitoring the integral ratios of ring N-H signal ( $\delta = 6.4\text{-}7.0$  ppm) at different time intervals. The ring N-H signal at  $t = 0$  was calculated based on the integral ratio of side-chain benzyl peaks between BLG-NCA ( $\delta = 5.17$  ppm) and resulting PBLG ( $\delta = 5.08$  ppm).

### **Simulation Methods**

Density functional theory (DFT) calculations were carried out in Gaussian 16 using the exchange-correlation functional of B3LYP and 6-311G(d,p) basis set in the presence of polarizable continuum model (PCM) describing DCM. Grimme's D3 dispersion correction was employed to improve the van der Waals interactions. Vibrational frequencies of each structure have been calculated to verify the presence of zero and single imaginary frequency for the intermediates and transition states, respectively. The reaction pathways of all TSs were checked by intrinsic reaction coordinate (IRC) calculations to confirm that these TSs were connected to the desired intermediates.

Thermal corrections to Gibbs free energies (G) were obtained in vacuum at 298.15 K and  $1.013 \times 10^5$  Pa.

## Supporting Figures

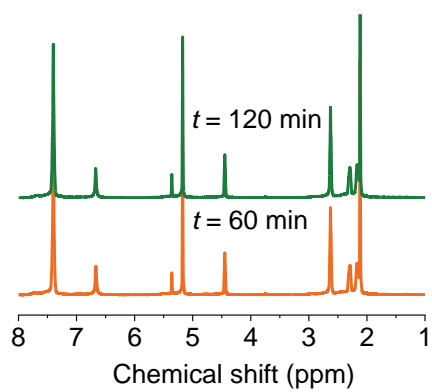


**Figure S1.** Overlaid NMR spectra (600 MHz) showing the stability of BLG-NCA in  $\text{CD}_2\text{Cl}_2$  in the presence of AcOH.  $[\text{M}]_0 = [\text{AcOH}]_0 = 0.1 \text{ M}$ .

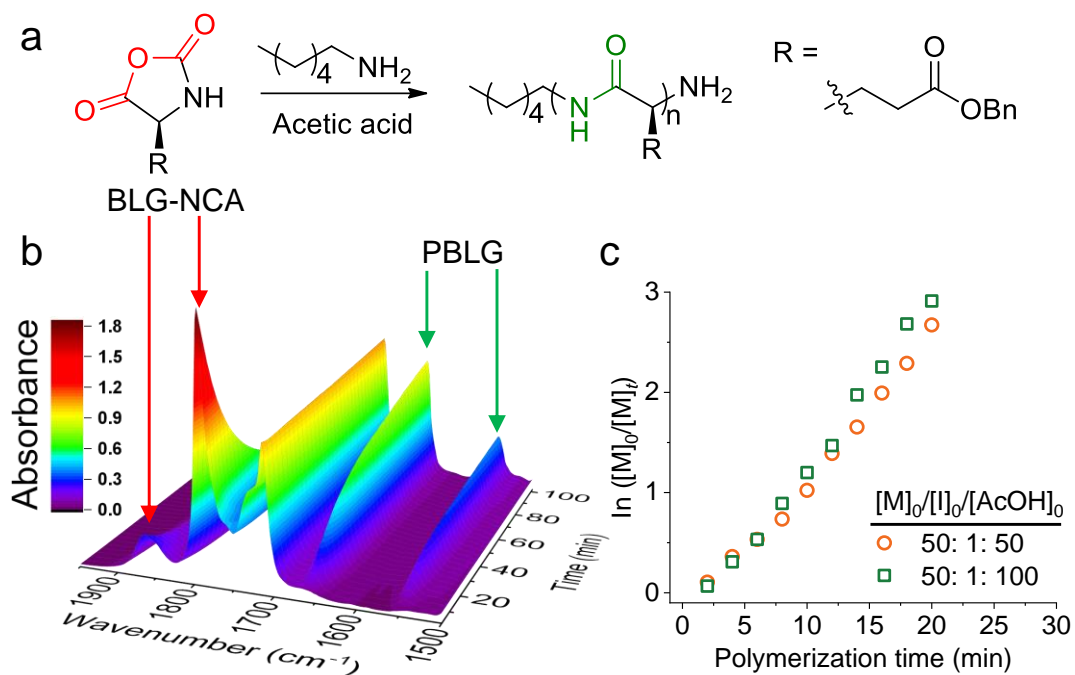


**Figure S2.** FTIR kinetic studies of NCA polymerization in the presence of AcOH. (a) Synthetic route to polypeptides through AcOH-accelerated polymerization of BLG-NCA. (b) Overlaid FTIR spectra showing the conversion of BLG-NCA initiated by Hex-NH<sub>2</sub> in the presence of AcOH in DCM.  $[M]_0/[I]_0/[AcOH]_0 = 100/1/100$ ,  $[M]_0 = 0.1$  M. (c) Semilogarithmic kinetic plot of polymerization of BLG-NCA in DCM initiated by Hex-NH<sub>2</sub> with different  $[AcOH]_0/[I]_0$  ratios.  $[M]_0/[I]_0 = 50$ ,  $[M]_0 = 0.1$  M.

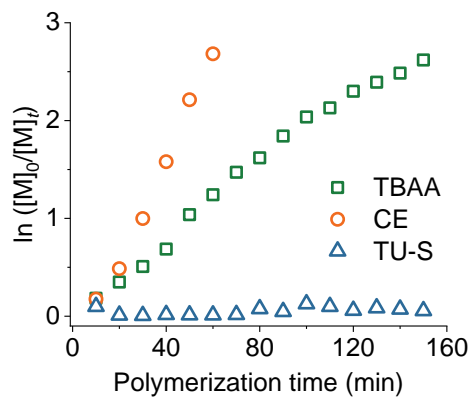


**Figure S3.** Semilogarithmic kinetic plot of polymerization of BLG-NCA in DCM in different catalytic systems. TBAA system:  $[M]_0/[TBAA]_0 = 100/1$ ,  $[M]_0 = 0.1$  M. 18-crown 6-ether (CE) system:  $[M]_0/[Hex-NH_2]_0/[CE]_0 = 100/1/1$ ,  $[M]_0 = 0.1$  M. TU-S system:  $[M]_0/[Hex-NH_2]_0/[TU-S]_0 = 100/1/1$ ,  $[M]_0 = 0.1$  M.



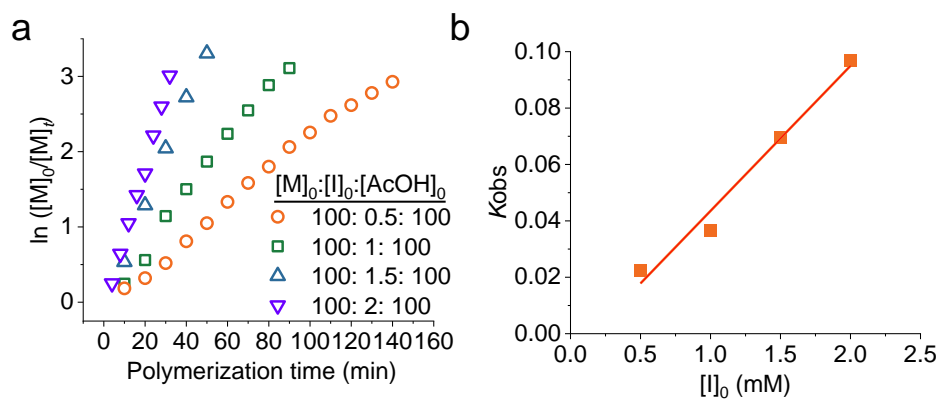


**Figure S4.** (a) Semilogarithmic kinetic plot of polymerization of BLG-NCA in DCM initiated by Hex-NH<sub>2</sub> with different  $[I]_0$ .  $[M]_0/[AcOH]_0 = 1$ ,  $[M]_0 = 0.1$  M. (b) The plots of  $K_{obs}$  obtained from (a) versus  $[I]_0$  and the linear fitting of the data.

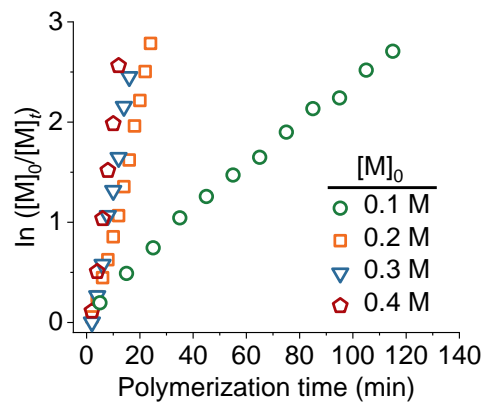


**Figure S5.** Semilogarithmic kinetic plot of polymerization of BLG-NCA in DCM initiated by Hex-NH<sub>2</sub> at various  $[M]_0$ .  $[M]_0/[I]_0 = 100$ .  $[M]_0/[AcOH]_0 = 1$ .

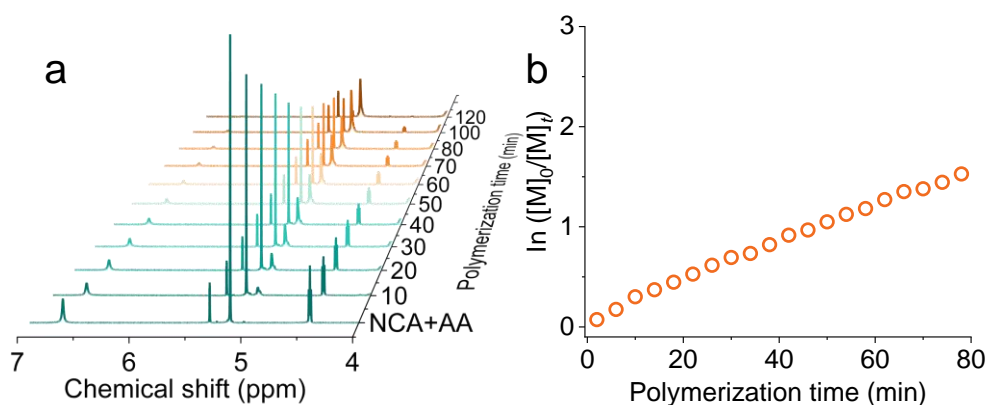


**Figure S6.** NMR kinetic studies of NCA polymerization in the presence of AcOH. (a) Overlaid  $^1\text{H}$  NMR spectra (600 MHz) showing the AcOH-accelerated polymerization of BLG-NCA in  $\text{CD}_2\text{Cl}_2$  initiated by Hex- $\text{NH}_2$ .  $[\text{M}]_0/[\text{I}]_0/[\text{AcOH}]_0 = 100/1/100$ ,  $[\text{M}]_0 = 0.1$  M. (b) Semilogarithmic kinetic plot of polymerization of BLG-NCA during the early stage of polymerization.

One-stage kinetics was observed with negligible transition as observed in conventional cooperative covalent polymerizations.

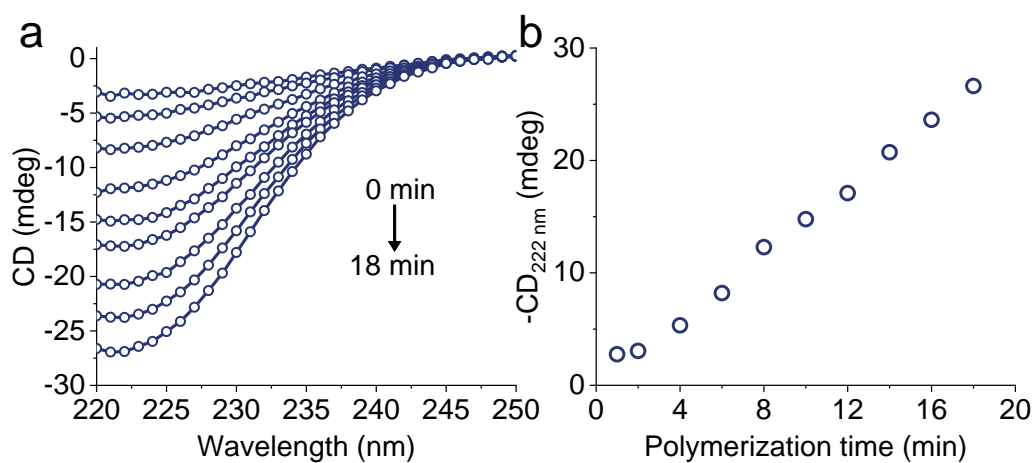


**Figure S7.** Secondary structure analysis during AcOH-accelerated polymerization. (a) Overlaid CD spectra of polymerization mixture quenched at different time intervals in DCM.  $[M]_0/[I]_0/[AcOH]_0 = 100/1/100$ ,  $[M]_0 = 0.1$  M. (b) The time-dependent change in CD signal at 222 nm over time during the early stage of polymerization.

The formation of random-coiled polypeptides at the early stage of the polymerization was verified by the initial slow increase in CD signal at 222 nm.

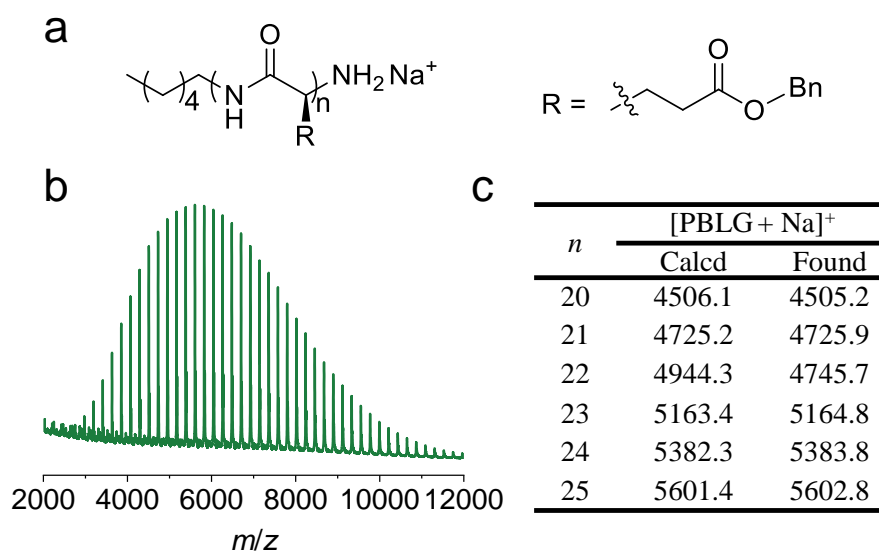


**Figure S8.** MALDI-TOF characterization of PBLG obtained from AcOH-accelerated polymerization. (a) Chemical structure of PBLG that were detected by MALDI-TOF. (b) MALDI-TOF spectrum of PBLG. (c) Comparison of representative *m/z* signals between calculated values from molecular formula and obtained values from MALDI-TOF spectrum.

The obtained *m/z* signals agree well with the calculated values of  $(124.11 + 219.1n)$  ( $[M + Na]^+$ ) and  $(140.11 + 219.1n)$  ( $[M + K]^+$ ), indicating negligible degradation of terminal amino groups.

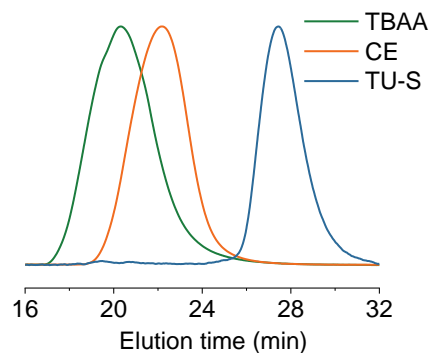


**Figure S9.** Normalized GPC-LS traces of the resulting polypeptides in different catalytic systems. TBAA system:  $[M]_0/[TBAA]_0 = 100/1$ ,  $[M]_0 = 0.1$  M. 18-crown 6-ether (CE) system:  $[M]_0/[Hex-NH_2]_0/[CE]_0 = 100/1/1$ ,  $[M]_0 = 0.1$  M. TU-S system:  $[M]_0/[Hex-NH_2]_0/[TU-S]_0 = 100/1/1$ ,  $[M]_0 = 0.1$  M.

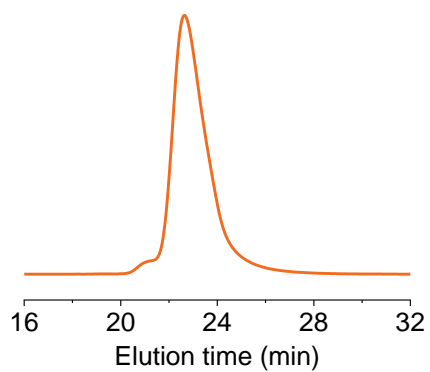


**Figure S10.** Normalized GPC-LS traces of the resulting polypeptides initiated by Hex-NH<sub>2</sub> in the presence of AcOH.  $[M]_0/[I]_0/[AcOH]_0 = 400/1/100$ ,  $[M]_0 = 0.4$  M.  $M_{n,GPC} = 92.6$  kDa,  $M_{n,theo.} = 87.6$  kDa,  $D = 1.13$ .

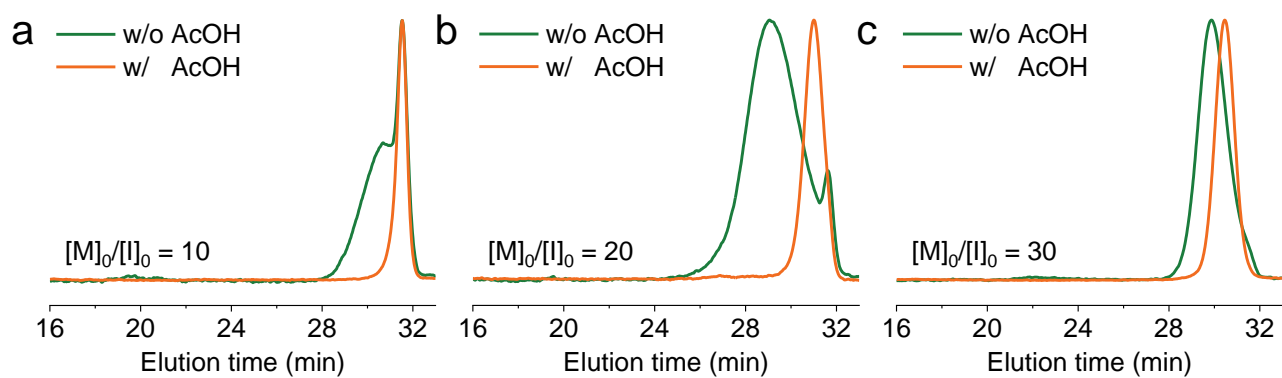


**Figure S11.** Normalized GPC-LS traces of obtained PBLG at low  $[M]_0/[I]_0 = 10$  (a), 20 (b), and 30 (c) in the presence and absence of AcOH.  $[M]_0 = 0.1$  M.



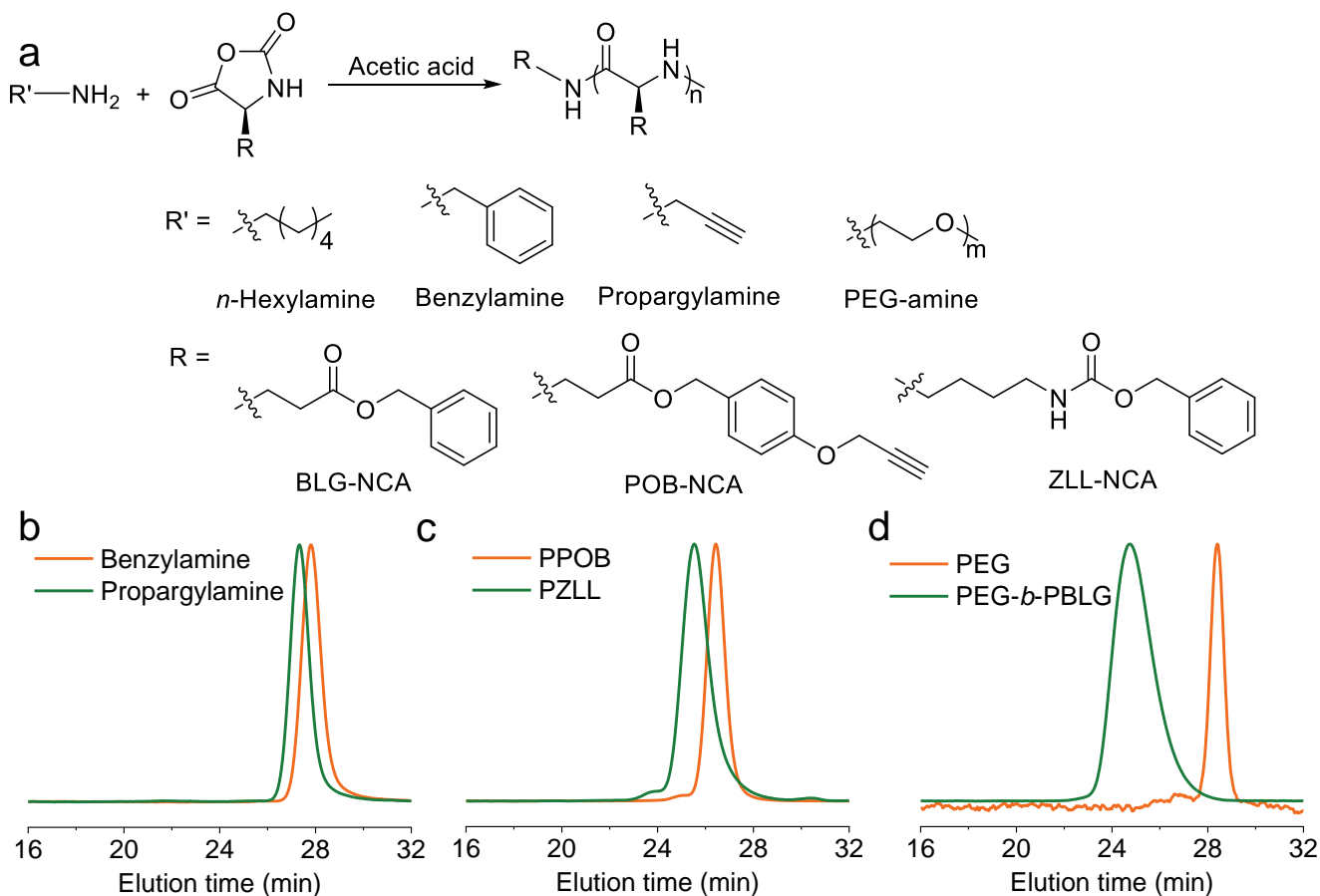


**Figure S12.** AcOH-catalyzed polymerization of various NCA monomers in the presence of different initiators. (a) Chemical structures of various initiators and NCA monomers. (b) Normalized GPC-LS traces of the resulting polypeptides initiated by benzylamine and propargylamine in the presence of AcOH. (c) Normalized GPC-LS traces of the resulting polypeptides obtained in the presence of AcOH with ZLL-NCA and POB-NCA as the monomer. (d) Normalized GPC-LS traces of the resulting polypeptides initiated by macroinitiator PEG-NH<sub>2</sub> (5 kDa) in the presence of AcOH.  $[M]_0/[I]_0/[AcOH]_0 = 100/1/100$ ,  $[M]_0 = 0.1$  M.

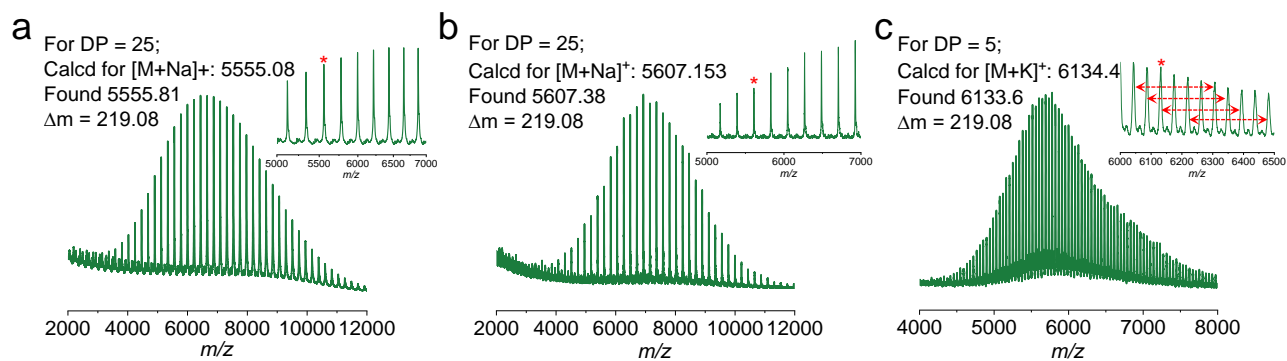


**Figure S13.** MALDI-TOF characterization of PBLG-NH<sub>2</sub>. MALDI-TOF spectra of PBLG-NH<sub>2</sub> initiated by (a) propagylamine, (b) benzylamine and (c) methoxy poly(ethylene glycol) (PEG) amine (5 kDa).

The obtained  $m/z$  signals for PBLG-NH<sub>2</sub> agree well with the calculated values, indicating the successful incorporation of the functional group at the C terminus.

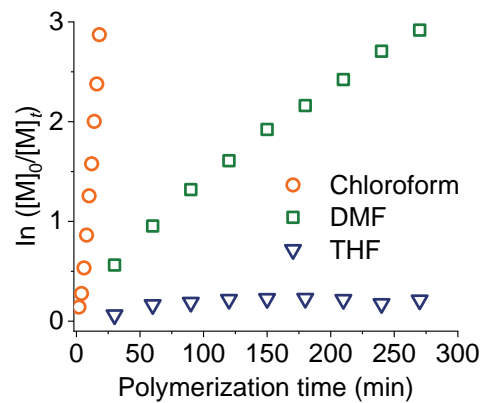


**Figure S14.** Semilogarithmic kinetic plot of polymerization of BLG-NCA in various solvents initiated by Hex-NH<sub>2</sub> in the presence of AcOH.  $[M]_0/[I]_0/[AcOH]_0 = 100/1/100$ ,  $[M]_0 = 0.1$  M.

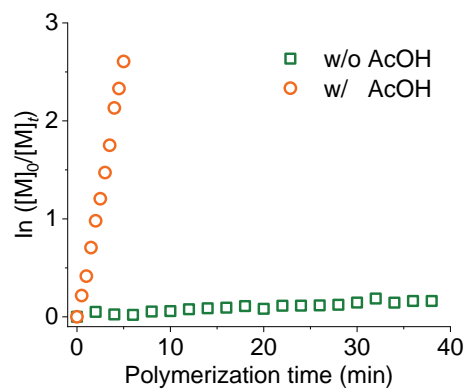


**Figure S15.** Semilogarithmic kinetic plot of ring-opening reaction of BLG-NCA by DBLG in DCM in the presence of AcOH.  $[M]_0/[DBLG]_0/[AcOH]_0 = 1/10/100$ ,  $[M]_0 = 0.1$  M.

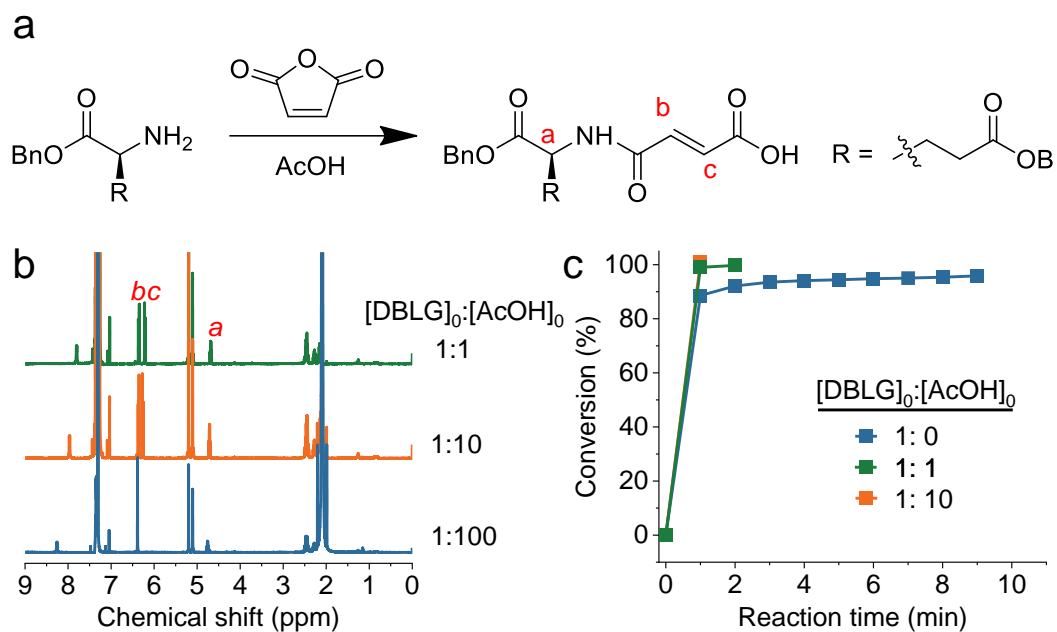


**Figure S16.** Ring-opening reaction of maleic anhydride (MA) in the presence of AcOH. (a) Chemical structures showing the ring-opening of MA by DBLG. (b) Overlaid  $^1\text{H}$  NMR spectra of polymerization of MA by DBLG in DCM with different  $[\text{DBLG}]_0/[\text{AcOH}]_0$  ratios. (c) Kinetic plot showing the consumption of MA at different  $[\text{DBLG}]_0/[\text{AcOH}]_0$  ratios.  $[\text{MA}]_0/[\text{DBLG}]_0 = 1$ .

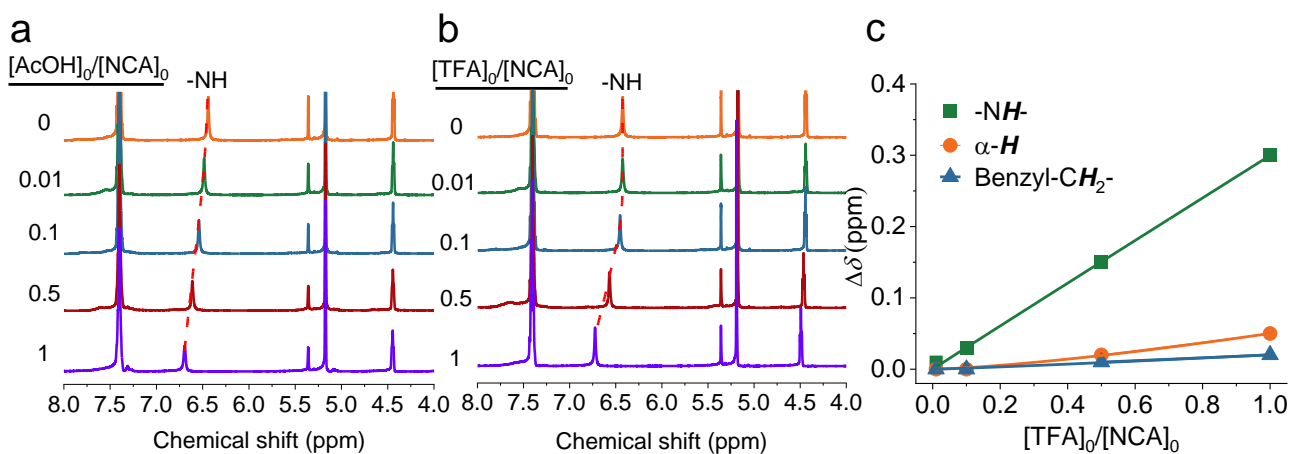


**Figure S17.** Quantification of fraction of BLG-NCA protonation through NMR titration. (a, b) Overlaid  $^1\text{H}$  NMR spectra of the mixture of BLG-NCA and (a) AcOH and (b) TFA in  $\text{CD}_2\text{Cl}_2$  at various  $[\text{acid}]_0/[\text{NCA}]_0$  ratios.  $[\text{NCA}]_0 = 0.1$  M. (c) The change in chemical shift of various protons in NCA at various  $[\text{TFA}]_0/[\text{NCA}]_0$  ratios.

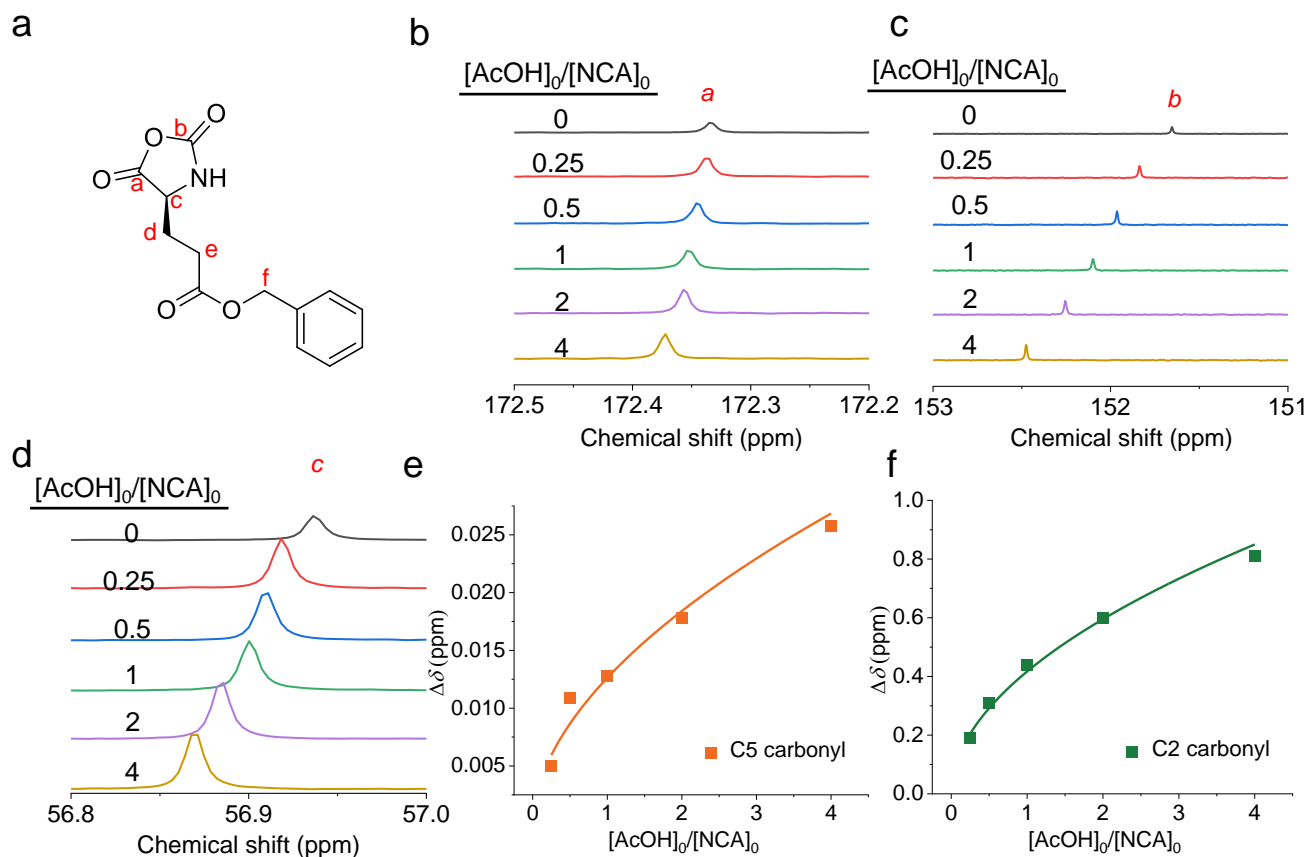


**Figure S18.** (a) Chemical structures of BLG-NCA. (b-d) Overlaid  $^{13}\text{C}$  NMR spectra of the mixture of BLG-NCA and AcOH in  $\text{CD}_2\text{Cl}_2$  at various concentrations of AcOH, with the molar ratios of AcOH to NCA ( $[\text{AcOH}]_0/[\text{NCA}]_0$  to be 0, 0.25, 0.5, 1, 2 and 4, respectively). (e) The change in chemical shift of  $\text{C}_5$ -carbon in NCA at various  $[\text{AcOH}]_0/[\text{NCA}]_0$  ratios.  $[\text{NCA}]_0 = 0.1 \text{ M}$ . (f) The change in chemical shift of  $\text{C}_2$ -carbon in NCA at various  $[\text{AcOH}]_0/[\text{NCA}]_0$  ratios.  $[\text{NCA}]_0 = 0.1 \text{ M}$ .

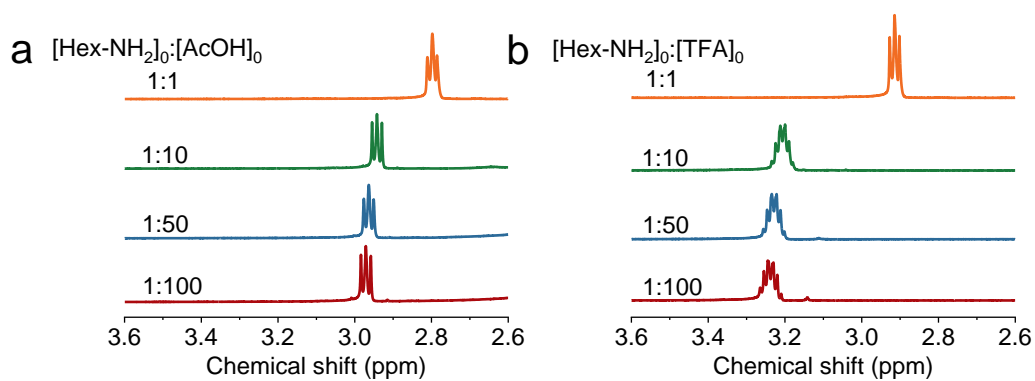


**Figure S19.** Detailed  $^1\text{H}$  NMR spectra showing the multiplicity of  $\alpha\text{-H}$  of Hex- $\text{NH}_2$  in the presence of AcOH (a) and TFA (b) in  $\text{CD}_2\text{Cl}_2$  at various  $[\text{Hex-NH}_2]_0/[\text{acid}]_0$  ratios.

A triplet peak of  $\alpha\text{-H}$  of Hex- $\text{NH}_2$  clearly changed to a multiplet peak corresponding to the complete protonation in the presence of TFA.



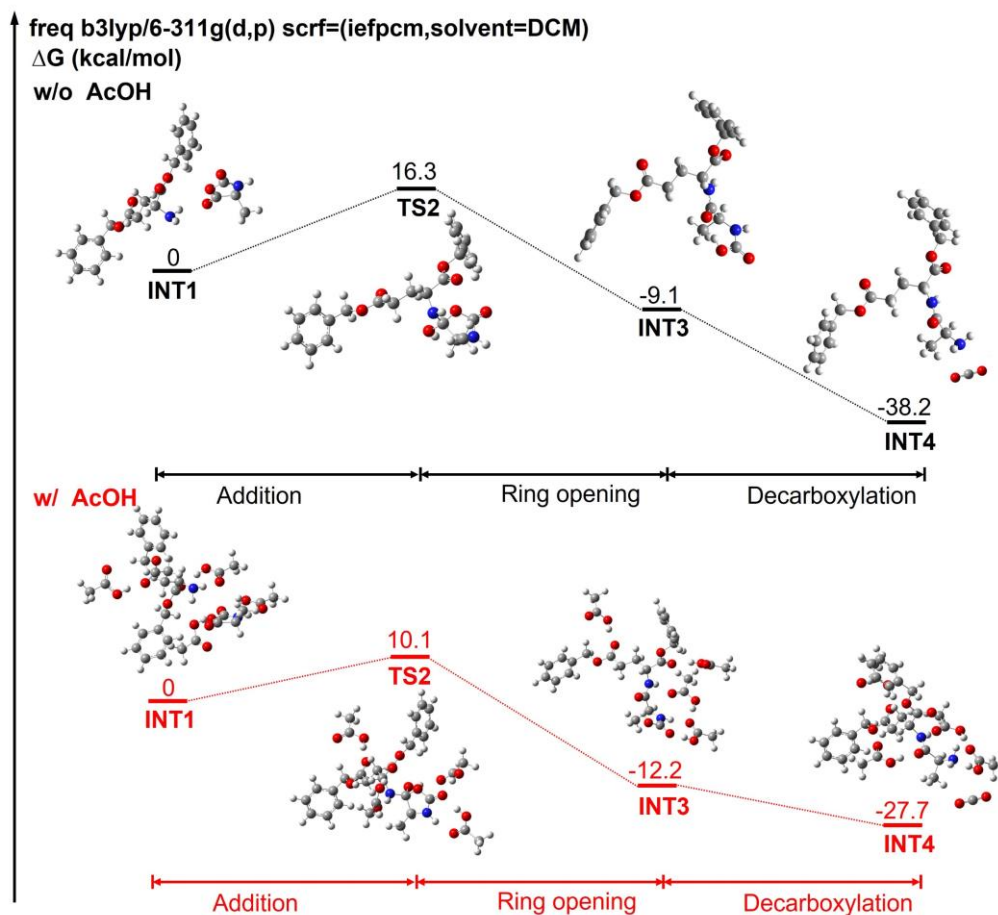


**Figure S20.** Calculated Gibbs free-energy profile of the model ring opening reaction in the absence (black) and presence (red) of AcOH. L-Alanine NCA was used as a model monomer for simplification. Some crucial intermediates (INT) and transition states (TS) are illustrated by 3D models where some hydrogen atoms are neglected for clarity.

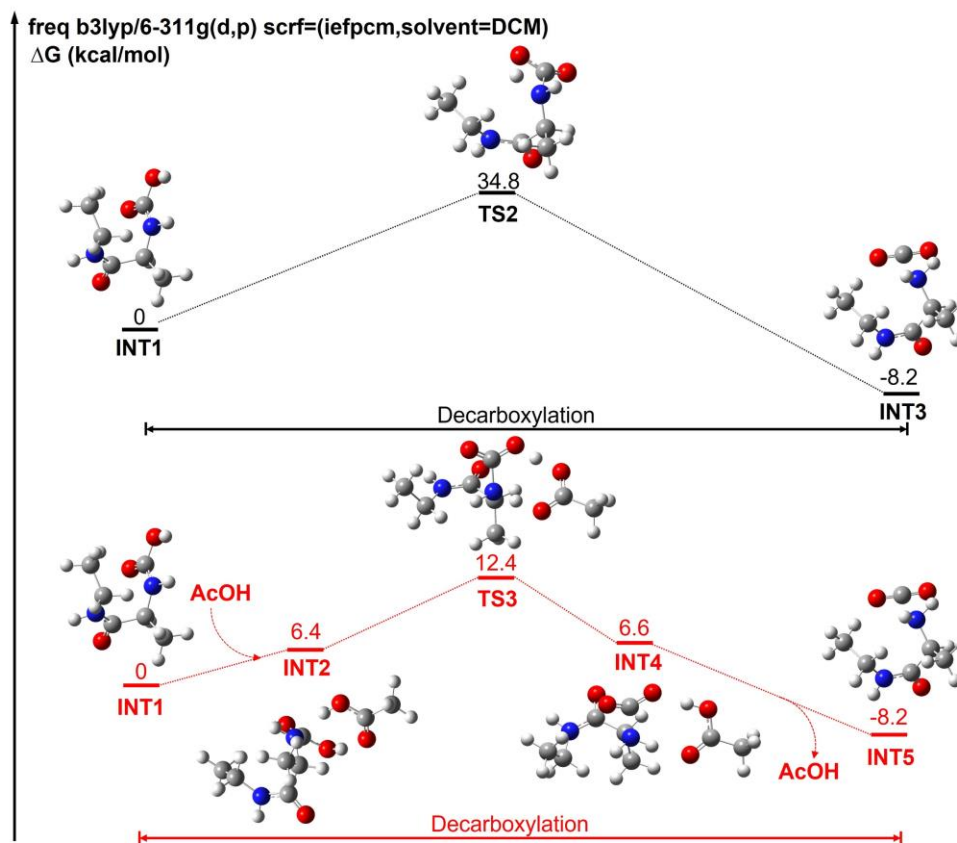


**Figure S21.** Calculated Gibbs free-energy profile of the model decarboxylation step in the absence (black) and presence (red) of AcOH. L-Alanine NCA was used as a model monomer for simplification. Some crucial intermediates (INT) and transition states (TS) are illustrated by 3D models where some hydrogen atoms are neglected for clarity.

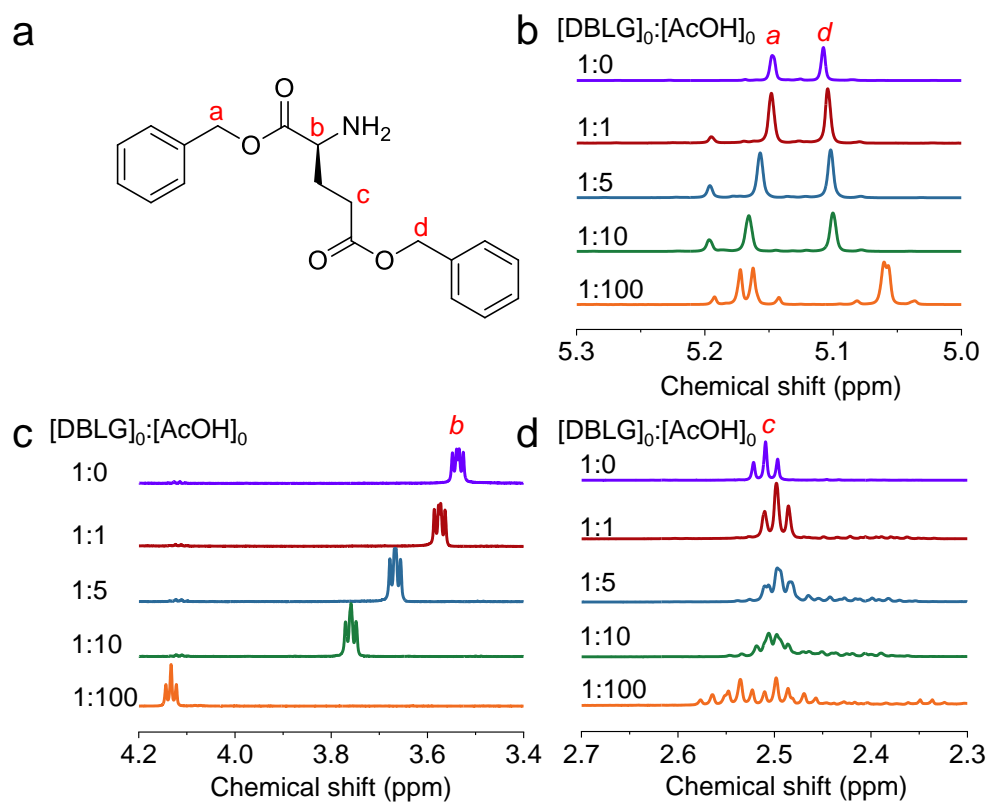


**Figure S22.** Molecular interactions between chain-end-mimicking DBLG and AcOH. (a) Chemical structures of DBLG. (b-d) Overlaid <sup>1</sup>H NMR spectra of the mixture of DBLG and AcOH in CDCl<sub>3</sub> at various [DBLG]<sub>0</sub>/[AcOH]<sub>0</sub> ratios. The benzyl protons (*a*), α-H (*b*), and γ-H (*c*) were highlighted with clear downfield shift, suggesting the binding interactions between AcOH and DBLG carbonyls.

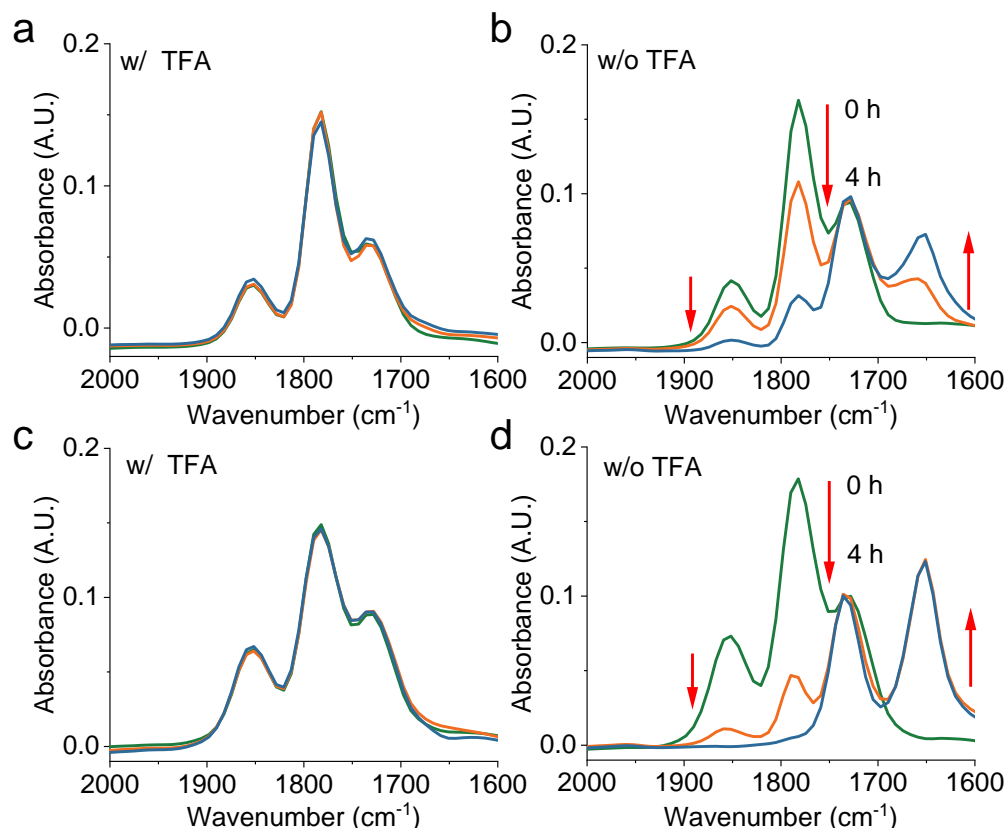


**Figure S23.** Water-induced degradation of NCA molecules. FTIR spectra showing the water-induced degradation of BLG-NCA in water/THF solution (a, b) or water/DCM biphasic mixture (c, d) (1 wt% water) in the absence and presence of TFA.  $[NCA]_0/[TFA]_0 = 1$ ,  $[NCA]_0 = 0.1$  M.

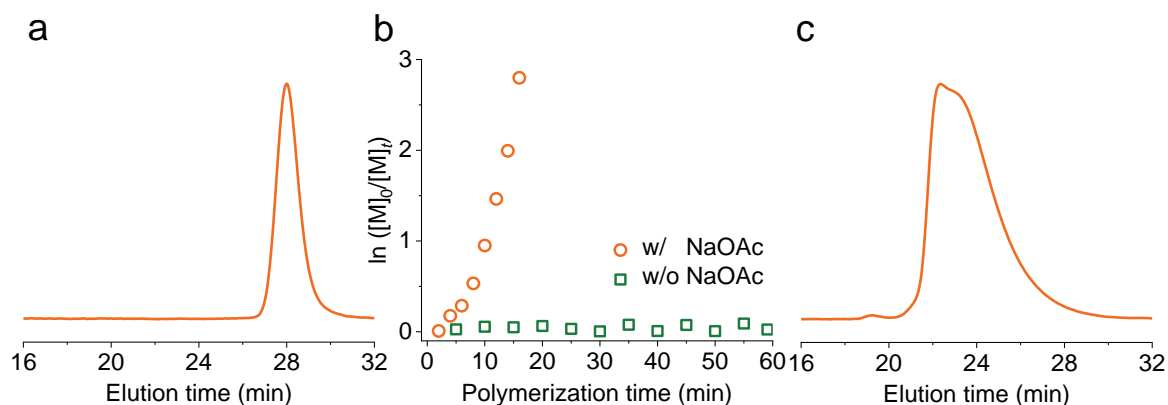


**Figure S24.** Polymerization of NCA in the presence of TFA and NaOAc. (a) GPC-LS traces of the obtained PBLG from purified NCA initiated by Hex-NH<sub>2</sub> in the presence TFA and NaOAc.  $[M]_0/[I]_0/[TFA]_0 = 100/1/100$ ,  $[M]_0 = [NaOAc]_0 = 0.1$  M.  $M_{n,GPC} = 21.5$  kDa,  $M_{n,theo.} = 21.9$  kDa,  $\mathcal{D} = 1.05$ . (b) Semilogarithmic kinetic plot of polymerization of non-purified BLG-NCA in DCM initiated by Hex-NH<sub>2</sub> in the absence and presence of NaOAc. (c) Normalized GPC-LS traces of the obtained PBLG initiated by Hex-NH<sub>2</sub> in the presence NaOAc.  $M_{n,GPC} = 51.9$  kDa,  $M_{n,theo.} = 21.9$  kDa,  $\mathcal{D} = 1.39$ . The broad distribution likely originated from the uncontrolled initiation from acetate anions.  $[M]_0/[I]_0/[NaOAc]_0 = 100/1/100$ ,  $[M]_0 = 0.1$  M

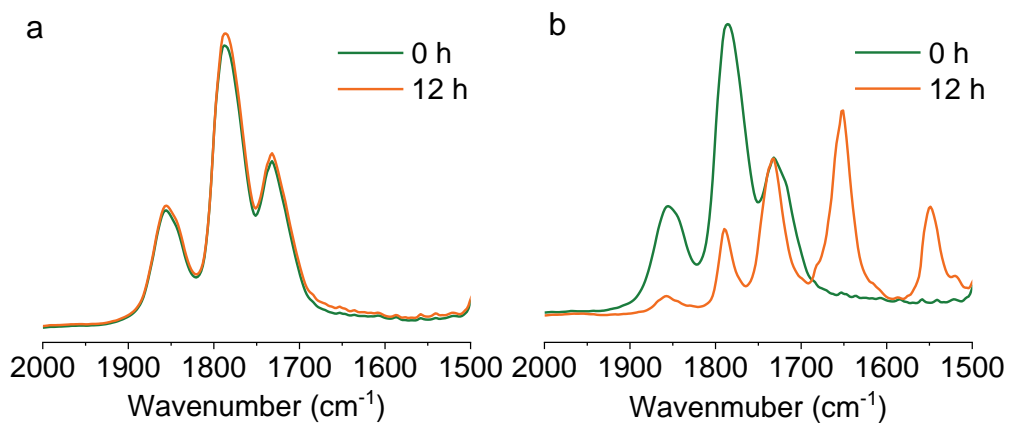


**Figure S25.** (a) Overlaid FTIR spectra showing the polymerization of non-purified BLG-NCA initiated by Hex-NH<sub>2</sub> after 12 h in DCM.  $[M]_0/[I]_0 = 100/1$ ,  $[M]_0 = 0.1$  M. (b) Overlaid FTIR spectra showing the polymerization of purified BLG-NCA initiated by Hex-NH<sub>2</sub> after 12 h in DCM.  $[M]_0/[I]_0 = 100/1$ ,  $[M]_0 = 0.1$  M.

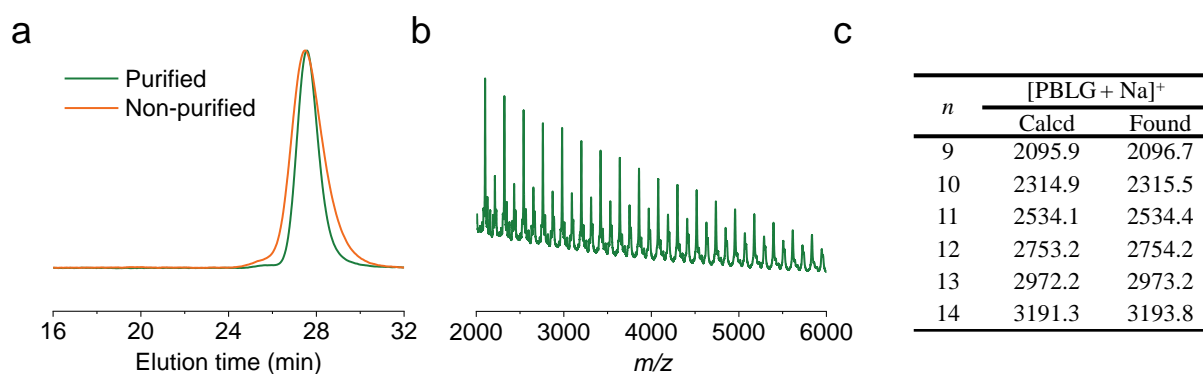


**Figure S26.** (a) Normalized GPC-LS traces of the resulting polypeptides obtained in the presence NaOAc with non-purified BLG-NCA and purified BLG-NCA as the monomer.  $[M]_0/[I]_0/[HCl]_0=100/1/100$ ,  $[M]_0=[NaOAc]_0 = 0.1$  M. (b) MALDI-TOF spectra of PBLG-NH<sub>2</sub> obtained in the presence NaOAc with non-purified BLG-NCA as the monomer. (c) Comparison of representative *m/z* signals between calculated values from molecular formula and obtained values from MALDI-TOF spectrum.

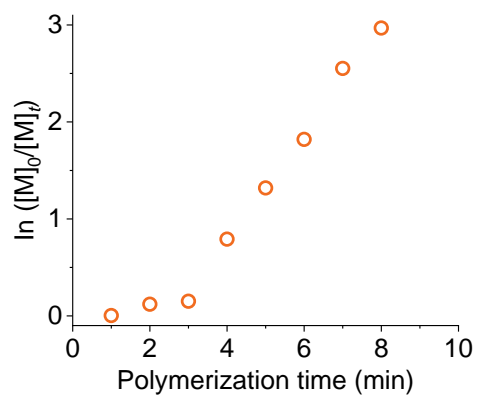


**Figure S27.** Semilogarithmic kinetic plot of polymerization of non-purified BLG-NCA in DCM initiated by Hex-NH<sub>2</sub> in the presence of HCl and NaOAc.



## Supporting Tables

**Table S1.** Characterization of resulting polypeptides from polymerization of BLG-NCAs in different catalytic systems.<sup>a</sup>

Entry	Catalytic systems	<i>t</i> (min) <sup>b</sup>	<i>M</i> <sub>n, GPC</sub> (kDa) <sup>c</sup>	<i>M</i> <sub>n, theo.</sub> (kDa)	<i>D</i> <sup>c</sup>
1	TBAA	60	214.9	21.9	1.89
2	CE	160	121.4	21.9	1.21
3	TU-S	2880	17.7	21.9	1.17

<sup>a</sup>All polymerization were conducted at room temperature in DCM using BLG-NCA as the monomer. TBAA system:  $[M]_0/[TBAA]_0 = 100/1$ ,  $[M]_0 = 0.1$  M. 18-crown 6-ether (CE) system:  $[M]_0/[Hex-NH_2]_0/[CE]_0 = 100/1/1$ ,  $[M]_0 = 0.1$  M. TU-S system:  $[M]_0/[Hex-NH_2]_0/[TU-S]_0 = 100/1/1$ ,  $[M]_0 = 0.1$  M. <sup>b</sup>Polymerization time reaching 95% monomer conversion. <sup>c</sup>Determined by GPC;  $dn/dc = 0.104$ .

**Table S2.** Characterization of resulting polypeptides from polymerization of BLG-NCAs at low  $[M]_0/[I]_0$  in the presence and absence of AcOH.<sup>a</sup>

Entry	$[M]_0/[I]_0/[AcOH]_0$	$t$ (min) <sup>b</sup>	$M_{n, GPC}$ (kDa) <sup>c</sup>	$M_{n, theo.}$ (kDa)	$\bar{D}$ <sup>c</sup>
1	10:1:0	360	2.91	2.19	1.31
2	20:1:0	480	4.35	4.38	1.36
3	30:1:0	600	6.48	6.57	1.21
4	10:1:100	30	2.48	2.19	1.05
5	20:1:100	30	4.21	4.38	1.07
6	30:1:100	45	6.53	6.57	1.06

<sup>a</sup>All polymerization were conducted at room temperature in DCM using Hex-NH<sub>2</sub> as the initiator and BLG-NCA as the monomer. <sup>b</sup>Polymerization time reaching 95% monomer conversion. <sup>c</sup>Determined by GPC;  $dn/dc = 0.104$ .

**Table S3.** Characterization of resulting polypeptides with various NCA monomers and initiators using AcOH as a catalyst.<sup>a</sup>

Entry	Initiator	Monomer	$t$ (min) <sup>b</sup>	$M_{n,\text{GPC}}$ (kDa) <sup>c</sup>	$M_{n,\text{theo.}}$ (kDa)	$\bar{D}$ <sup>c</sup>
1	Propargylamine	BLG-NCA	120	23.9	21.9	1.05
2	Benzylamine	BLG-NCA	120	20.8	21.9	1.05
3	<i>n</i> -Hexylamine	ZLL-NCA	90	30.4	26.2	1.07
4	<i>n</i> -Hexylamine	POB-NCA	120	27.2	26.8	1.05

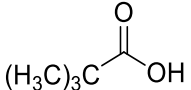
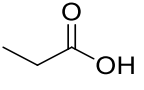
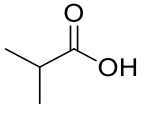
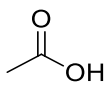
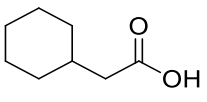
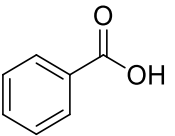
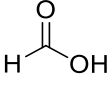
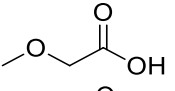
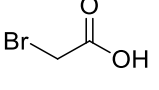
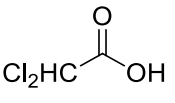
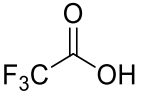
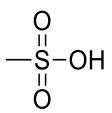
<sup>a</sup>All polymerizations were conducted at room temperature in DCM.  $[M]_0/[I]_0/[AcOH]_0 = 100/1/100$ . <sup>b</sup>Polymerization time reaching 95% monomer conversion. <sup>c</sup>Determined by GPC; the  $dn/dc$  value of PBLG, PZLL, and PPOB was 0.104, 0.123, and 0.1, respectively.

**Table S4.** Characterization of block copolypeptides using AcOH as a catalyst.<sup>a</sup>

Block No.	Monomer	$[M]_0/[I]_0$	$t$ (min) <sup>b</sup>	$M_{n, \text{GPC}}$ (kDa) <sup>c</sup>	$M_{n, \text{theo.}}$ (kDa)	$\mathcal{D}^c$
1	BLG-NCA	50	60	11.1	10.9	1.05
2	ELG-NCA	50	30	24.1	22.3	1.06

<sup>a</sup>All polymerizations were conducted at room temperature in DCM.  $[M]_0 = [AcOH]_0 = 0.1$  M. <sup>b</sup>Polymerization time reaching 95% monomer conversion. <sup>c</sup>Determined by GPC;  $dn/dc = 0.104$ .

**Table S5.** Conversion of BLG-NCA monomer in the presence of various organic acid after 4 h.<sup>a</sup>

Entry	Organic acid	Chemical structure	pK <sub>a</sub>	Conversion (%)
1	Trimethylacetic acid		5.03	97
2	Propanoic acid		4.87	95
3	Isobutyric acid		4.84	96
4	Acetic acid		4.76	99
5	Cyclohexylacetic acid		4.51	98
6	Benzoic acid		4.2	72
7	Formic acid		3.77	33
8	Methoxyacetic acid		3.53	22
9	Bromoacetic acid		2.90	15
10	Dichloroacetic acid		1.35	1
11	Trifluoroacetic acid		0.52	2
12	Methanesulfonic acid		-1.2	1

<sup>a</sup>All polymerization were conducted at room temperature in DCM using Hex-NH<sub>2</sub> as the initiator. [M]<sub>0</sub> = 0.1 M.

**Table S6.** Characterization of resulting PBLG in different solvents initiated by Hex-NH<sub>2</sub>.<sup>a</sup>

Entry	Solvent	<i>t</i> (min) <sup>b</sup>	<i>M</i> <sub>n,GPC</sub> (kDa) <sup>c</sup>	<i>D</i> <sup>c</sup>
1	DMF	480	29.8	1.24
2	Chloroform	30	19.1	1.05
3	THF	2880	21.0	1.36

<sup>a</sup>All polymerizations were conducted at room temperature in DCM with BLG-NCA as the monomer. The theoretical MW was 21.9 kDa.  $[M]_0/[I]_0/[AcOH]_0 = 100/1/100$ .  $[M]_0 = 0.1$  M. <sup>b</sup>Polymerization time reaching 95% monomer conversion. <sup>c</sup>Determined by GPC;  $dn/dc = 0.104$ .

**Table S7.** Chlorine analysis in non-purified BLG NCA<sup>a</sup> and purified BLG NCA<sup>b</sup>

Entry	NCA	Chlorine content (%) <sup>c</sup>
1	Non-purified	1.02
2	Purified	0.01

<sup>a</sup>The reaction mixture was dried under vacuum without any additional purification procedures. <sup>b</sup>The reaction mixture was purified by triple recrystallization. <sup>c</sup>Chlorine content is the weight of chlorine per gram of BLG NCA.

**Table S8.** Characterization of resulting polypeptides with various non-purified monomers.<sup>a</sup>

Entry	Monomer	$[M]_0/[I]_0$	$t$ (min) <sup>b</sup>	$M_{n, \text{GPC}}$ (kDa) <sup>c</sup>	$M_{n, \text{theo.}}$ (kDa)	$\bar{D}$ <sup>c</sup>
1	BLG-NCA	50	10	10.8	10.9	1.09
2	BLG-NCA	100	15	21.3	21.9	1.06
3	BLG-NCA	150	40	30.7	32.8	1.05
4	BLG-NCA	200	60	44.4	43.8	1.05
5	ZLL-NCA	100	15	36.1	26.2	1.07
6	ELG-NCA	100	15	12.7	15.7	1.05

<sup>a</sup>All polymerizations were conducted at room temperature in DCM using Hex-NH<sub>2</sub> as the initiator.  $[M]_0/[I]_0/[HCl]_0/[NaOAc]_0 = 100/1/100/100$ . <sup>b</sup>Polymerization time reaching 95% monomer conversion. <sup>c</sup>Determined by GPC; the  $dn/dc$  value of PBLG, PZLL, and PELG was 0.104, 0.123, and 0.072, respectively.



## Cartesian Coordinates of the optimized geometries

### w/o AcOH INT1

C	-0.119	-0.315	1.876
H	-0.602	-0.515	2.836
N	0.181	-1.612	1.253
H	0.681	-2.208	1.905
C	1.161	0.445	2.229
O	1.647	0.491	3.336
O	1.723	1.017	1.148
C	2.998	1.675	1.35
H	3.731	0.913	1.628
H	2.911	2.378	2.179
C	3.395	2.379	0.078
C	3.106	1.838	-1.18
C	4.108	3.579	0.151
C	3.524	2.488	-2.339
H	2.541	0.917	-1.248
C	4.536	4.223	-1.008
H	4.328	4.014	1.121
C	4.244	3.68	-2.258
H	3.287	2.063	-3.308
H	5.087	5.154	-0.934
H	4.568	4.184	-3.161
C	-1.067	0.503	0.988
C	-2.426	-0.179	0.839
H	-0.614	0.642	0.004
H	-1.196	1.502	1.416
H	-2.278	-1.223	0.543
H	-2.973	-0.203	1.785
C	-3.306	0.465	-0.207
O	-2.931	1.2	-1.093
O	-4.593	0.097	-0.049
C	-5.538	0.616	-1.032
H	-5.23	0.274	-2.021

H	-5.491	1.706	-1.013
C	-6.904	0.109	-0.666
C	-7.368	-1.11	-1.171
C	-7.721	0.837	0.204
C	-8.625	-1.592	-0.814
H	-6.742	-1.681	-1.849
C	-8.979	0.357	0.563
H	-7.371	1.785	0.599
C	-9.433	-0.859	0.054
H	-8.975	-2.537	-1.215
H	-9.605	0.933	1.236
H	-10.413	-1.232	0.33
O	3.93	-1.504	0.386
C	5.326	-1.661	0.569
O	5.896	-1.132	1.479
C	3.523	-2.175	-0.733
N	5.769	-2.455	-0.425
H	6.75	-2.665	-0.529
C	4.733	-2.85	-1.365
C	4.551	-4.361	-1.524
H	4.898	-2.389	-2.345
H	4.375	-4.835	-0.557
H	3.701	-4.558	-2.178
O	2.384	-2.195	-1.097
H	0.781	-1.495	0.439
H	5.444	-4.798	-1.974

**w/o AcOH TS2**

C	-0.705	0.755	1.556
H	-0.253	0.831	2.552
N	-0.69	2.141	1.041
H	-1.185	2.722	1.704
C	-2.161	0.333	1.846
O	-2.923	1.061	2.443
O	-2.469	-0.889	1.408

C	-3.852	-1.334	1.589
H	-4.493	-0.455	1.553
H	-3.929	-1.788	2.578
C	-4.176	-2.314	0.497
C	-4.472	-1.853	-0.792
C	-4.176	-3.688	0.747
C	-4.764	-2.758	-1.81
H	-4.475	-0.787	-0.997
C	-4.472	-4.594	-0.271
H	-3.947	-4.052	1.744
C	-4.765	-4.129	-1.552
H	-4.994	-2.393	-2.805
H	-4.473	-5.658	-0.065
H	-4.996	-4.831	-2.345
C	0.121	-0.245	0.744
C	1.601	0.134	0.704
H	-0.27	-0.332	-0.268
H	0.005	-1.225	1.21
H	1.729	1.12	0.251
H	2.026	0.2	1.71
C	2.436	-0.841	-0.092
O	2.014	-1.752	-0.766
O	3.749	-0.56	0.033
C	4.666	-1.416	-0.712
H	4.423	-1.343	-1.773
H	4.512	-2.447	-0.392
C	6.064	-0.945	-0.426
C	6.654	0.047	-1.215
C	6.786	-1.476	0.648
C	7.941	0.501	-0.937
H	6.102	0.463	-2.052
C	8.074	-1.024	0.928
H	6.337	-2.248	1.264
C	8.653	-0.034	0.136
H	8.39	1.268	-1.558

H	8.625	-1.446	1.761
H	9.657	0.316	0.351
O	-2.321	1.557	-0.619
C	-3.287	2.3	-1.236
O	-4.319	1.822	-1.644
C	-1.154	2.391	-0.277
N	-2.856	3.587	-1.312
H	-3.489	4.311	-1.614
C	-1.667	3.856	-0.514
C	-1.97	4.701	0.723
H	-0.908	4.36	-1.117
H	-2.708	4.22	1.37
H	-1.06	4.898	1.294
O	-0.13	2.047	-1.166
H	-0.478	2.058	-2.067
H	-2.376	5.665	0.41

**w/o AcOH INT3**

C	-1.35	0.585	-0.54
H	-1.407	0.644	0.548
N	-0.774	1.835	-1.023
H	-1.071	2.132	-1.943
C	-2.766	0.477	-1.103
O	-3.172	1.127	-2.039
O	-3.471	-0.445	-0.449
C	-4.838	-0.687	-0.927
H	-4.778	-1.035	-1.958
H	-5.372	0.264	-0.907
C	-5.465	-1.707	-0.023
C	-5.405	-3.067	-0.339
C	-6.099	-1.31	1.159
C	-5.97	-4.016	0.511
H	-4.917	-3.383	-1.255
C	-6.664	-2.256	2.01
H	-6.154	-0.256	1.41

C	-6.599	-3.612	1.687
H	-5.921	-5.068	0.254
H	-7.156	-1.938	2.922
H	-7.041	-4.349	2.347
C	-0.531	-0.659	-0.947
C	0.876	-0.669	-0.354
H	-0.476	-0.708	-2.039
H	-1.076	-1.545	-0.616
H	1.464	0.188	-0.694
H	0.843	-0.596	0.738
C	1.642	-1.927	-0.705
O	1.187	-2.89	-1.279
O	2.916	-1.842	-0.284
C	3.759	-3.008	-0.536
H	3.776	-3.195	-1.611
H	3.308	-3.87	-0.041
C	5.129	-2.707	0
C	6.103	-2.135	-0.823
C	5.441	-2.974	1.337
C	7.368	-1.835	-0.321
H	5.871	-1.927	-1.862
C	6.705	-2.675	1.842
H	4.692	-3.42	1.983
C	7.67	-2.104	1.013
H	8.117	-1.395	-0.97
H	6.936	-2.889	2.879
H	8.655	-1.874	1.404
O	0.987	4.751	1.881
C	0.406	5.644	1.069
O	0.297	6.813	1.383
C	-0.103	2.692	-0.237
N	-0.088	5.162	-0.13
H	-0.486	5.9	-0.691
C	0.376	3.993	-0.893
C	1.899	3.949	-1.107

H	-0.105	4.086	-1.867
H	2.427	3.874	-0.156
H	2.171	3.09	-1.724
O	0.164	2.443	0.947
H	0.754	3.821	1.614
H	2.221	4.859	-1.617
C	-1.35	0.585	-0.54
H	-1.407	0.644	0.548

**w/o AcOH INT4**

C	-1.339	1.251	-0.183
H	-1.341	1.075	0.894
N	-0.857	2.604	-0.401
H	-1.181	3.063	-1.241
C	-2.776	1.157	-0.695
O	-3.286	1.957	-1.445
O	-3.381	0.059	-0.231
C	-4.749	-0.179	-0.699
H	-4.727	-0.254	-1.786
H	-5.356	0.683	-0.419
C	-5.239	-1.444	-0.056
C	-5.039	-2.679	-0.68
C	-5.881	-1.405	1.186
C	-5.474	-3.856	-0.074
H	-4.544	-2.718	-1.645
C	-6.317	-2.58	1.793
H	-6.043	-0.45	1.675
C	-6.113	-3.808	1.164
H	-5.317	-4.808	-0.568
H	-6.817	-2.538	2.754
H	-6.455	-4.723	1.635
C	-0.471	0.176	-0.875
C	0.955	0.136	-0.332
H	-0.452	0.37	-1.951
H	-0.949	-0.796	-0.733

H	1.443	1.11	-0.434
H	0.97	-0.096	0.737
C	1.821	-0.879	-1.047
O	1.495	-1.523	-2.018
O	3.029	-0.975	-0.462
C	3.968	-1.913	-1.069
H	4.143	-1.605	-2.101
H	3.509	-2.903	-1.076
C	5.231	-1.888	-0.257
C	6.259	-0.994	-0.57
C	5.386	-2.744	0.838
C	7.422	-0.955	0.196
H	6.148	-0.328	-1.42
C	6.548	-2.707	1.607
H	4.595	-3.443	1.088
C	7.568	-1.811	1.286
H	8.214	-0.259	-0.059
H	6.659	-3.377	2.451
H	8.474	-1.784	1.881
C	-0.281	3.353	0.577
N	-0.09	5.733	1.301
H	-1.076	5.793	1.544
C	0.08	4.799	0.186
C	1.533	4.836	-0.306
H	-0.577	5.124	-0.627
H	2.208	4.503	0.488
H	1.678	4.188	-1.173
O	-0.019	2.911	1.692
H	1.799	5.859	-0.579
H	0.364	5.329	2.117
C	-1.339	1.251	-0.183
H	-1.341	1.075	0.894
N	-0.857	2.604	-0.401
H	-1.181	3.063	-1.241
C	-2.776	1.157	-0.695

w/ AcOH INT1

C	-0.73	-0.623	0.807
H	-0.768	-1.435	1.537
N	-0.291	-1.201	-0.47
H	0.562	-1.74	-0.328
C	0.324	0.35	1.332
O	1.224	0.037	2.096
O	0.218	1.568	0.81
C	1.28	2.528	1.129
H	2.237	2.039	0.947
H	1.21	2.773	2.189
C	1.083	3.737	0.262
C	1.321	3.663	-1.116
C	0.659	4.948	0.815
C	1.136	4.781	-1.924
H	1.645	2.725	-1.555
C	0.481	6.072	0.007
H	0.469	5.013	1.881
C	0.717	5.989	-1.363
H	1.322	4.713	-2.99
H	0.154	7.007	0.448
H	0.578	6.86	-1.992
C	-2.12	0.013	0.679
C	-3.177	-1.029	0.317
H	-2.094	0.795	-0.082
H	-2.385	0.502	1.621
H	-2.856	-1.588	-0.568
H	-3.305	-1.769	1.112
C	-4.528	-0.434	0.01
O	-4.725	0.746	-0.224
O	-5.485	-1.363	0.002
C	-6.842	-0.927	-0.345
H	-6.805	-0.478	-1.339
H	-7.154	-0.17	0.375



C	-7.73	-2.137	-0.313
C	-7.792	-3.002	-1.41
C	-8.495	-2.424	0.822
C	-8.602	-4.134	-1.374
H	-7.205	-2.785	-2.297
C	-9.308	-3.555	0.86
H	-8.456	-1.756	1.676
C	-9.362	-4.412	-0.238
H	-8.644	-4.796	-2.232
H	-9.9	-3.765	1.743
H	-9.995	-5.291	-0.21
O	3.491	0.058	-0.932
C	4.609	-0.7	-0.629
O	5.18	-0.562	0.444
C	3.005	-0.327	-2.169
N	4.891	-1.51	-1.642
H	5.682	-2.157	-1.576
C	3.926	-1.402	-2.727
C	3.188	-2.702	-3.056
H	4.403	-0.999	-3.627
H	2.725	-3.112	-2.158
H	2.421	-2.503	-3.805
O	2.018	0.149	-2.637
H	-0.08	-0.464	-1.139
O	5.957	2.451	-0.587
O	5.099	2.046	1.451
H	5.108	1.119	1.121
C	5.627	4.292	0.94
H	4.609	4.641	1.13
H	6.088	4.906	0.169
H	6.184	4.382	1.875
C	5.593	2.853	0.496
O	7.131	-3.094	-0.904
O	7.228	-2.266	1.186
H	6.505	-1.669	0.874

C	8.767	-3.966	0.63
H	9.626	-3.352	0.907
H	9.036	-4.636	-0.182
H	8.479	-4.541	1.513
C	7.631	-3.077	0.209
H	3.89	-3.431	-3.465
O	2.354	-2.672	0.369
O	2.433	-2.324	2.587
H	1.904	-1.516	2.368
C	3.687	-4.136	1.746
H	4.674	-3.736	1.99
H	3.762	-4.771	0.866
H	3.343	-4.712	2.606
C	2.755	-2.984	1.478
O	-7.678	2.038	1.246
O	-6.478	2.831	-0.482
H	-5.952	2.009	-0.346
C	-8.252	4.18	0.296
H	-7.596	5.038	0.461
H	-9.062	4.188	1.021
H	-8.654	4.266	-0.716
C	-7.46	2.904	0.424

**w/ AcOH TS2**

C	-0.039	-0.491	1.724
H	-0.372	-1.071	2.589
N	0.635	-1.492	0.877
H	1.038	-2.221	1.459
C	0.966	0.511	2.311
O	1.739	0.23	3.212
O	0.927	1.707	1.743
C	1.929	2.682	2.164
H	2.904	2.287	1.869
H	1.904	2.769	3.25
C	1.619	3.99	1.492

C	1.42	4.052	0.108
C	1.551	5.166	2.242
C	1.156	5.271	-0.511
H	1.46	3.141	-0.479
C	1.299	6.389	1.621
H	1.695	5.126	3.317
C	1.099	6.443	0.244
H	0.995	5.306	-1.582
H	1.25	7.295	2.215
H	0.896	7.392	-0.24
C	-1.273	0.165	1.089
C	-2.295	-0.876	0.641
H	-0.979	0.785	0.247
H	-1.724	0.825	1.836
H	-1.852	-1.56	-0.089
H	-2.628	-1.505	1.473
C	-3.524	-0.272	0.006
O	-3.659	0.912	-0.249
O	-4.445	-1.199	-0.255
C	-5.682	-0.753	-0.907
H	-5.411	-0.304	-1.865
H	-6.148	0.006	-0.279
C	-6.56	-1.957	-1.087
C	-6.416	-2.782	-2.207
C	-7.523	-2.279	-0.125
C	-7.218	-3.909	-2.364
H	-5.674	-2.536	-2.96
C	-8.327	-3.407	-0.28
H	-7.644	-1.642	0.744
C	-8.175	-4.224	-1.399
H	-7.1	-4.539	-3.238
H	-9.073	-3.645	0.47
H	-8.803	-5.099	-1.522
O	2.753	-0.463	0.256
C	3.763	-0.934	-0.476

O	4.885	-0.396	-0.465
C	1.453	-1.145	-0.203
N	3.396	-1.992	-1.2
H	4.066	-2.446	-1.823
C	2.007	-2.381	-0.998
C	1.876	-3.754	-0.342
H	1.479	-2.383	-1.954
H	2.362	-3.789	0.635
H	0.826	-4.025	-0.223
O	0.819	-0.221	-1.005
H	1.477	0.237	-1.561
O	2.743	1.244	-2.444
O	4.771	1.98	-1.816
H	4.773	1.165	-1.255
C	3.613	3.268	-3.417
H	3.607	4.17	-2.802
H	2.724	3.243	-4.042
H	4.511	3.3	-4.037
C	3.648	2.06	-2.522
O	5.669	-2.918	-2.704
O	7.044	-1.449	-1.699
H	6.212	-1.122	-1.262
C	8.019	-2.97	-3.215
H	8.489	-2.161	-3.778
H	7.76	-3.788	-3.884
H	8.741	-3.312	-2.47
C	6.785	-2.457	-2.525
H	2.349	-4.5	-0.985
O	1.495	-3.307	3.083
O	2.285	-1.963	4.701
H	2.023	-1.237	4.081
C	2.429	-4.288	5.074
H	3.514	-4.272	5.202
H	2.124	-5.238	4.641
H	1.982	-4.162	6.061

C	2.016	-3.155	4.174
O	-6.901	2.243	0.324
O	-5.26	2.997	-1.015
H	-4.799	2.177	-0.72
C	-7.171	4.364	-0.794
H	-6.587	5.224	-0.458
H	-8.157	4.384	-0.335
H	-7.262	4.435	-1.88
C	-6.457	3.09	-0.422

**w/ AcOH INT3**

C	0.044	0.398	0.494
H	-0.069	0.426	1.577
N	0.665	-0.876	0.156
H	1.057	-0.987	-0.777
C	0.964	1.543	0.075
O	1.745	1.46	-0.852
O	0.764	2.622	0.814
C	1.533	3.832	0.465
H	1.265	4.107	-0.556
H	2.592	3.579	0.503
C	1.163	4.901	1.45
C	0.07	5.74	1.21
C	1.898	5.06	2.629
C	-0.285	6.72	2.134
H	-0.503	5.626	0.295
C	1.545	6.04	3.554
H	2.75	4.417	2.82
C	0.452	6.87	3.308
H	-1.133	7.367	1.937
H	2.123	6.157	4.464
H	0.179	7.635	4.026
C	-1.331	0.584	-0.183
C	-2.351	-0.453	0.282
H	-1.21	0.529	-1.268

H	-1.693	1.588	0.049
H	-2.003	-1.47	0.078
H	-2.511	-0.399	1.363
C	-3.696	-0.295	-0.39
O	-3.934	0.518	-1.265
O	-4.584	-1.162	0.088
C	-5.934	-1.135	-0.493
H	-5.84	-1.336	-1.561
H	-6.345	-0.135	-0.354
C	-6.747	-2.187	0.203
C	-6.737	-3.509	-0.253
C	-7.512	-1.861	1.327
C	-7.477	-4.489	0.403
H	-6.15	-3.769	-1.128
C	-8.254	-2.84	1.985
H	-7.53	-0.837	1.684
C	-8.237	-4.155	1.524
H	-7.465	-5.51	0.039
H	-8.847	-2.575	2.853
H	-8.816	-4.917	2.034
O	2.661	-3.101	3.36
C	3.532	-3.196	2.356
O	4.724	-3.412	2.605
C	0.977	-1.793	1.087
N	3.081	-3.052	1.087
H	3.815	-3.017	0.381
C	1.698	-3.051	0.592
C	0.914	-4.319	0.956
H	1.799	-2.993	-0.489
H	0.796	-4.428	2.034
H	-0.08	-4.286	0.504
O	0.71	-1.665	2.292
H	1.833	-2.629	3.075
O	2.5	-1.614	-2.136
O	4.587	-1.557	-2.957

H	4.81	-2.069	-2.14
C	2.926	-0.423	-4.19
H	3.324	0.584	-4.042
H	1.844	-0.374	-4.295
H	3.378	-0.835	-5.093
C	3.29	-1.257	-2.993
O	5.356	-2.907	-0.708
O	6.692	-3.664	0.917
H	5.876	-3.567	1.509
C	7.678	-3.314	-1.2
H	8.294	-2.437	-0.982
H	7.387	-3.291	-2.248
H	8.277	-4.2	-0.988
C	6.464	-3.28	-0.316
H	1.441	-5.193	0.571
O	-7.128	2.059	-1.08
O	-5.766	1.804	-2.851
H	-5.216	1.303	-2.208
C	-7.71	3.105	-3.175
H	-7.137	3.965	-3.529
H	-8.606	3.443	-2.659
H	-7.984	2.513	-4.051
C	-6.862	2.279	-2.244
O	4.867	3.082	-0.309
O	3.996	2.24	-2.201
H	3.202	2.111	-1.635
C	6.266	2.892	-2.267
H	6.582	1.906	-2.615
H	7.044	3.337	-1.652
H	6.088	3.509	-3.15
C	4.995	2.761	-1.471

**w/ AcOH INT4**

C	1.208	1.055	0.191
H	0.988	1.486	1.17

N	2.116	-0.065	0.375
H	2.113	-0.799	-0.33
C	1.88	2.148	-0.649
O	2.95	2.048	-1.2
O	1.112	3.246	-0.686
C	1.627	4.375	-1.461
H	1.788	4.039	-2.486
H	2.588	4.667	-1.035
C	0.619	5.484	-1.385
C	-0.401	5.581	-2.336
C	0.673	6.422	-0.349
C	-1.351	6.598	-2.255
H	-0.449	4.86	-3.145
C	-0.274	7.439	-0.265
H	1.463	6.355	0.392
C	-1.289	7.528	-1.218
H	-2.135	6.665	-3
H	-0.22	8.163	0.541
H	-2.025	8.321	-1.155
C	-0.109	0.588	-0.454
C	-0.881	-0.37	0.455
H	0.101	0.102	-1.41
H	-0.716	1.47	-0.664
H	-0.264	-1.241	0.703
H	-1.141	0.104	1.403
C	-2.135	-0.91	-0.188
O	-2.331	-0.942	-1.391
O	-2.993	-1.375	0.718
C	-4.229	-1.992	0.222
H	-3.95	-2.843	-0.403
H	-4.756	-1.261	-0.39
C	-5.033	-2.418	1.415
C	-4.847	-3.682	1.984
C	-5.966	-1.547	1.986
C	-5.58	-4.07	3.103



H	-4.128	-4.366	1.545
C	-6.7	-1.932	3.106
H	-6.12	-0.567	1.549
C	-6.508	-3.194	3.667
H	-5.43	-5.054	3.534
H	-7.424	-1.25	3.538
H	-7.081	-3.496	4.536
C	3.076	-0.086	1.313
N	5.393	-0.864	0.919
H	5.377	-0.297	0.074
C	4.018	-1.294	1.265
C	4.024	-2.027	2.605
H	3.698	-1.969	0.471
H	4.316	-1.349	3.411
H	3.031	-2.42	2.833
O	3.237	0.804	2.16
O	1.789	-2.273	-1.523
O	2.929	-3.672	-2.861
H	3.701	-3.434	-2.284
C	0.637	-3.37	-3.331
H	0.822	-3.032	-4.353
H	-0.254	-2.885	-2.939
H	0.493	-4.452	-3.367
C	1.827	-3.04	-2.471
O	5.042	-3.063	-1.324
O	6.728	-3.044	0.134
H	6.254	-2.19	0.463
C	6.703	-4.811	-1.44
H	7.627	-4.536	-1.955
H	6.03	-5.297	-2.143
H	6.969	-5.494	-0.632
C	6.069	-3.566	-0.879
H	4.727	-2.861	2.572
O	-5.706	-0.398	-2.459
O	-3.994	-1.401	-3.515

H	-3.52	-1.229	-2.669
C	-5.987	-1.111	-4.747
H	-5.475	-0.571	-5.547
H	-7.006	-0.745	-4.646
H	-5.993	-2.168	-5.019
C	-5.242	-0.921	-3.451
O	0.011	1.726	3.223
O	1.992	1.904	4.269
H	2.348	1.543	3.419
C	0.074	2.517	5.5
H	0.331	1.838	6.316
H	-1.007	2.596	5.409
H	0.5	3.493	5.74
C	0.663	2.008	4.21
H	5.765	-0.273	1.659

## Supporting References

- 1 Tian, Z.; Zhang, Z.; Wang, S.; Lu, H. A moisture-tolerant route to unprotected  $\alpha/\beta$ -amino acid *N*-carboxyanhydrides and facile synthesis of hyperbranched polypeptides. *Nat. Commun.* **12**, 5810 (2021).
- 2 Zhang, R.; Zheng, N.; Song, Z.; Yin, L.; Cheng, J. The effect of side-chain functionality and hydrophobicity on the gene delivery capabilities of cationic helical polypeptides. *Biomaterials* **35**, 3443-3454 (2014).
- 3 Xia, Y.; Song, Z.; Tan, Z.; Xue, T.; Wei, S.; Zhu, L.; Yang, Y.; Fu, H.; Jiang, Y.; Lin, Y.; Lu, Y.; Ferguson, A. L.; Cheng, J. Accelerated polymerization of *N*-carboxyanhydrides catalyzed by crown ether. *Nat. Commun.* **12**, 732 (2021).